Supplement of Atmos. Chem. Phys., 22, 12961–12983, 2022
https://doi.org/10.5194/acp-22-12961-2022-supplement

Atmospheric Chemistry and Physics
Open Access
EGU

Supplement of

Assessment of NAAPS-RA performance in Maritime Southeast Asia during CAMP^{2}Ex

Eva-Lou Edwards et al.

Correspondence to: Armin Sorooshian (armin@arizona.edu)

Table S1. Dates for each research flight (RF) based on UTC time at takeoff.

RF	Date
1	24 August 2019
2	27 August 2019
3	29 August 2019
4	30 August 2019
5	4 September 2019
6	6 September 2019
7	8 September 2019
8	13 September 2019
9	15 September 2019
10	16 September 2019
11	19 September 2019
12	21 September 2019
13	23 September 2019
14	25 September 2019
15	27 September 2019
16	29 September 2019
17	1 October 2019
18	3 October 2019
19	5 October 2019

Table S2. Summary statistics (means [standard deviations in parentheses] and number of points [N]) for mixed layer heights (MLHs) for each RF determined from the High Spectral Resolution Lidar (HSRL-2) MLH product.

RF	Mean (m)	N
1	543.77 (111.26)	186
2	615.46 (103.02)	485
3	629.20 (197.64)	440
4	519.01 (223.01)	706
5	502.74 (256.55)	985
6	611.89 (119.66)	518
7	513.37 (307.58)	742
8	560.08 (217.53)	965
9	637.81 (120.17)	1042
10	593.43 (128.65)	374
11	589.08 (202.78)	262
12	654.84 (136.63)	1332
13	662.46 (117.20)	1049
14	691.20 (174.78)	562
15	504.54 (170.50)	1069
16	491.21 (109.85)	620
17	534.80 (123.50)	1102
18	572.84 (198.32)	430
19	578.75 (136.55)	569

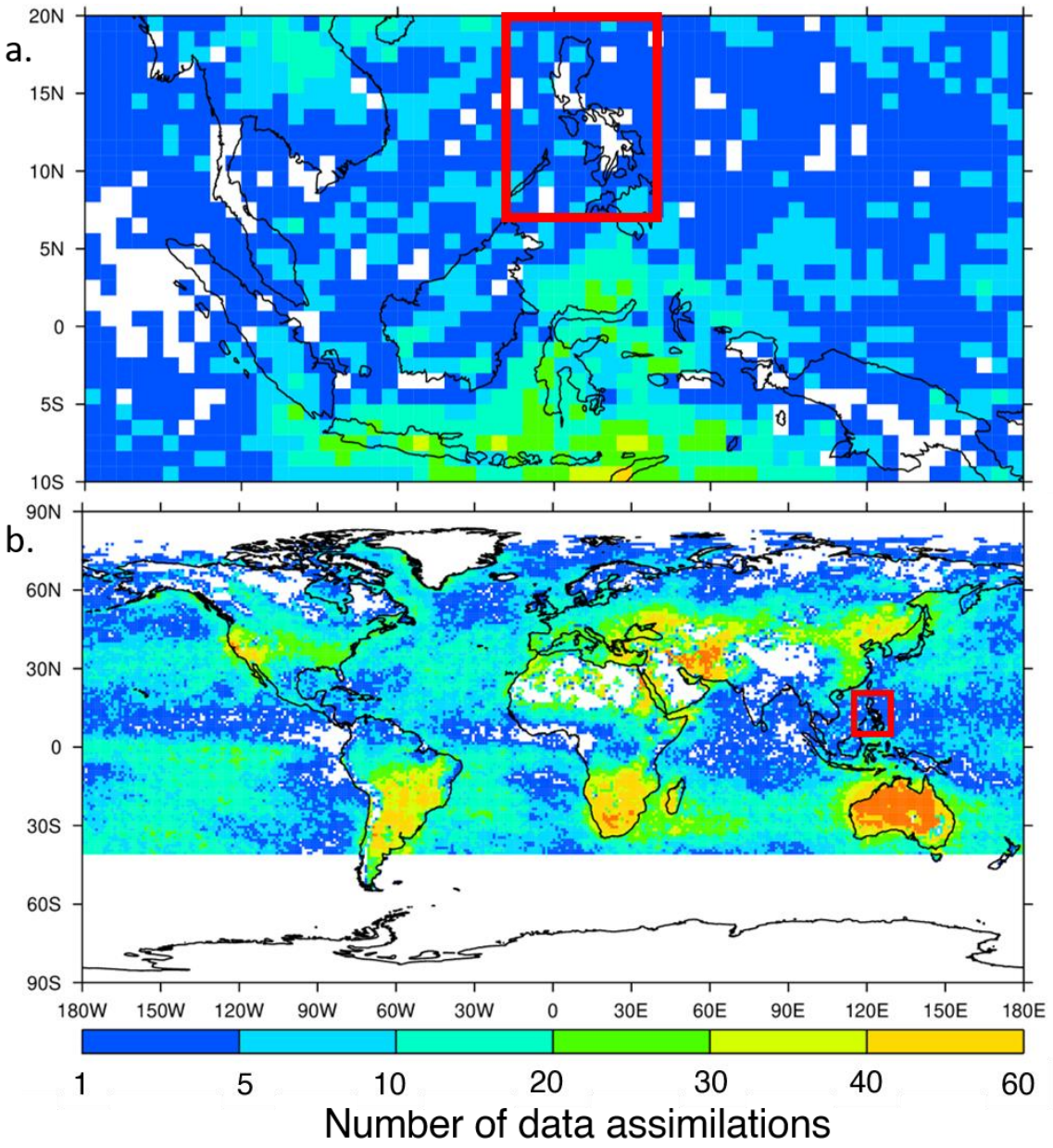

Figure S1. Total number of quality-controlled and assured MODIS AOT retrievals that were assimilated into NAAPS-RA per 1° × 1° grid cell during the time period relevant to the campaign (00Z 24 August 2019 – 18Z 04 October 2019) for (**a)** Southeast Asia and (**b**) the entire globe. White grid cells indicate there were zero data assimilations, and red rectangles indicate the region in which we evaluated NAAPS-RA performance.

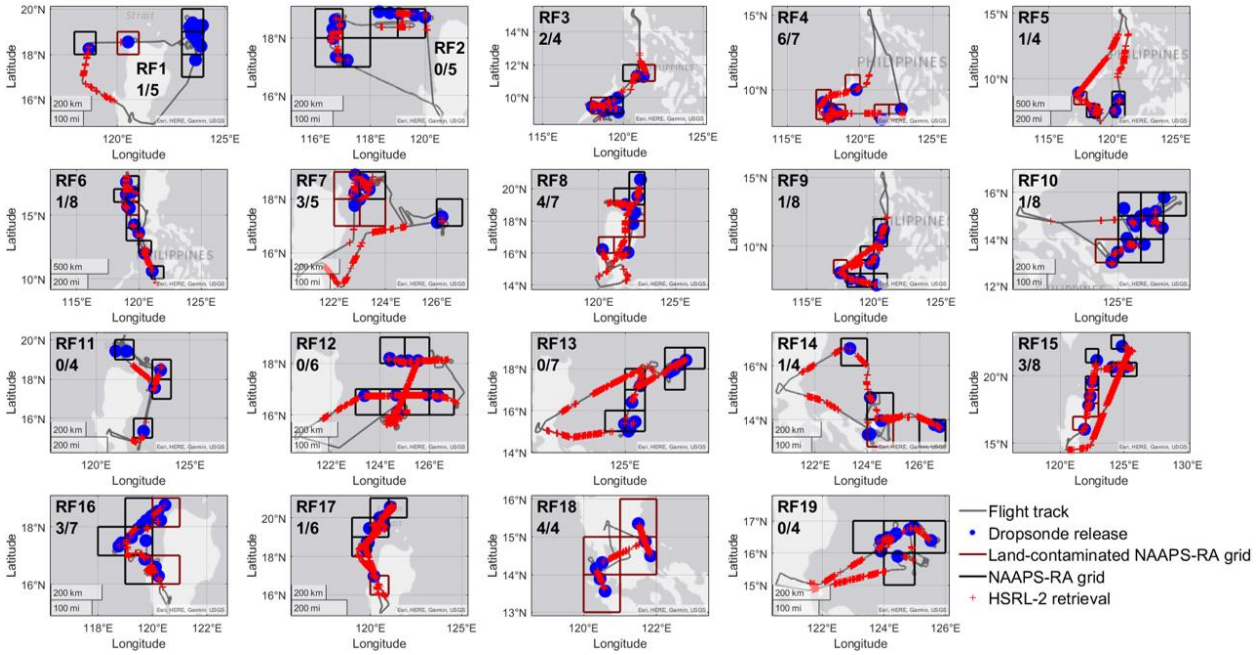

Figure S2. Flight tracks (grey lines), dropsonde release points (blue circles), and 1° × 1° grid cells relevant to NAAPS-RA data (outlined with black squares). NAAPS-RA grid cells encompassing land at the surface (outlined with maroon squares) were eliminated from the study. The number of eliminated grid cells out of the total is then reported for each research flight (RF).

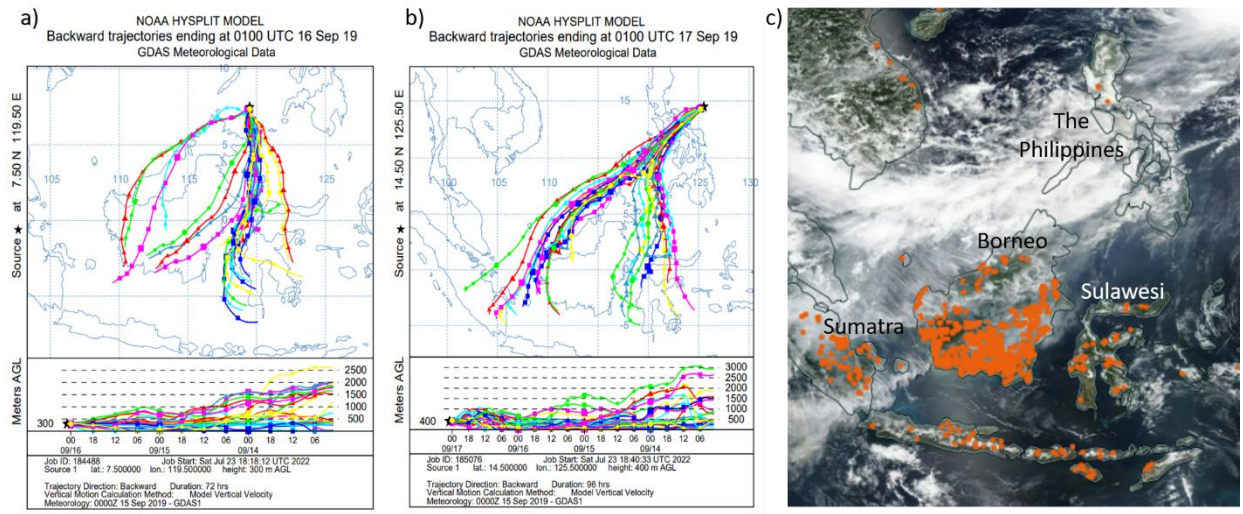

Figure S3. Information regarding the source and age of the smoke sampled during Cases II and III. (**a**) 72-hour and (**b**) 96-hour back-trajectories from the Hybrid Single Particle Lagrangian Integrated Trajectory (HYSPLIT) model (Rolph et al., 2017; Stein et al., 2015) ending at the center of the 1° × 1° grid cell chosen for Case II and Case III, respectively, and at the midpoint hour when the aircraft sampled the mixed layer within each grid cell. The "ensemble" feature was selected when running the HYSPLIT model so that each trajectory was calculated for the same end point and end time but the meteorological data was offset by a fixed grid cell factor. (**c**) Moderate Resolution Imaging Spectroradiometer (MODIS) true-color image and fires (orange dots) on the day (14 September 2019) the back-trajectories in (**a**) and (**b**) passed over locations conducting seasonal biomass burning.

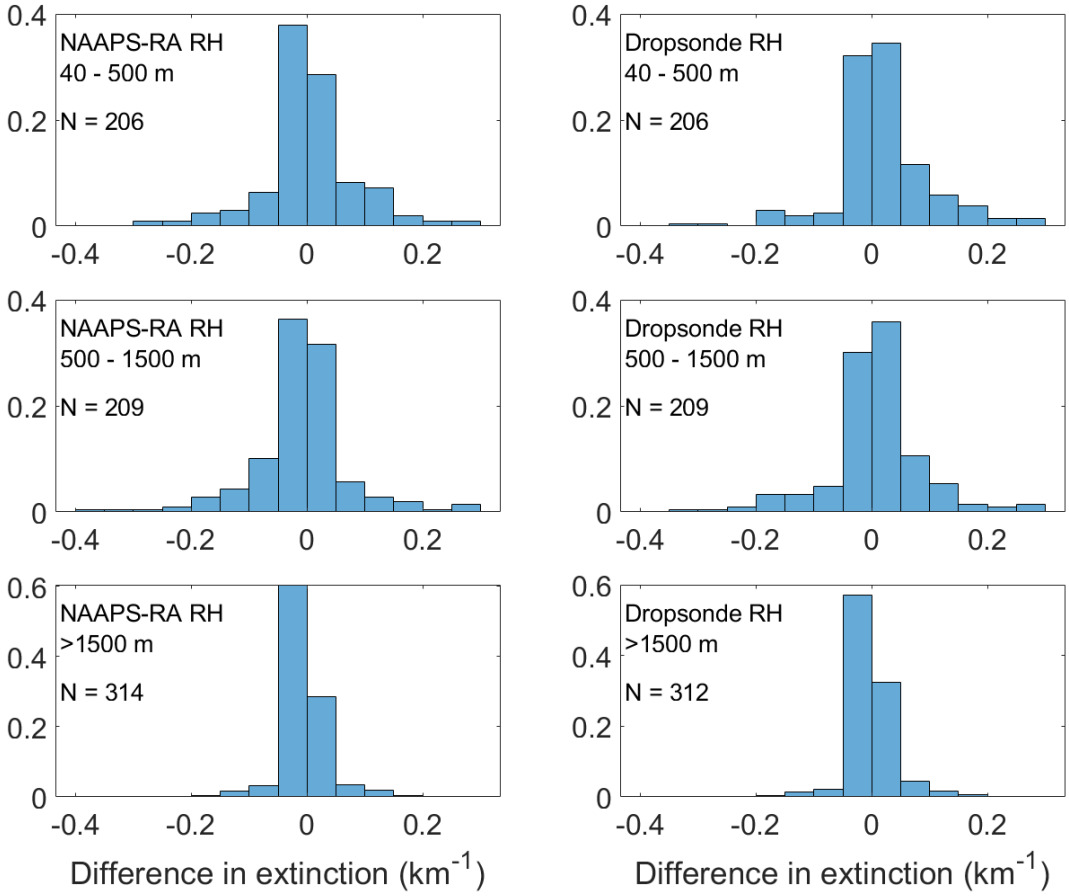

Figure S4. Normalized histograms of differences between simulated (NAAPS-RA) and retrieved (HSRL-2) 532 nm extinction coefficients for alititudes of (top) 40 – 500 m, (center) 500 – 1500 m, and (bottom) > 1500 m. Panels on the left are based on NAAPS-RA simulations using modeled relative humidities (RHs), and panels on the right are based on simulations using dropsonde RHs.

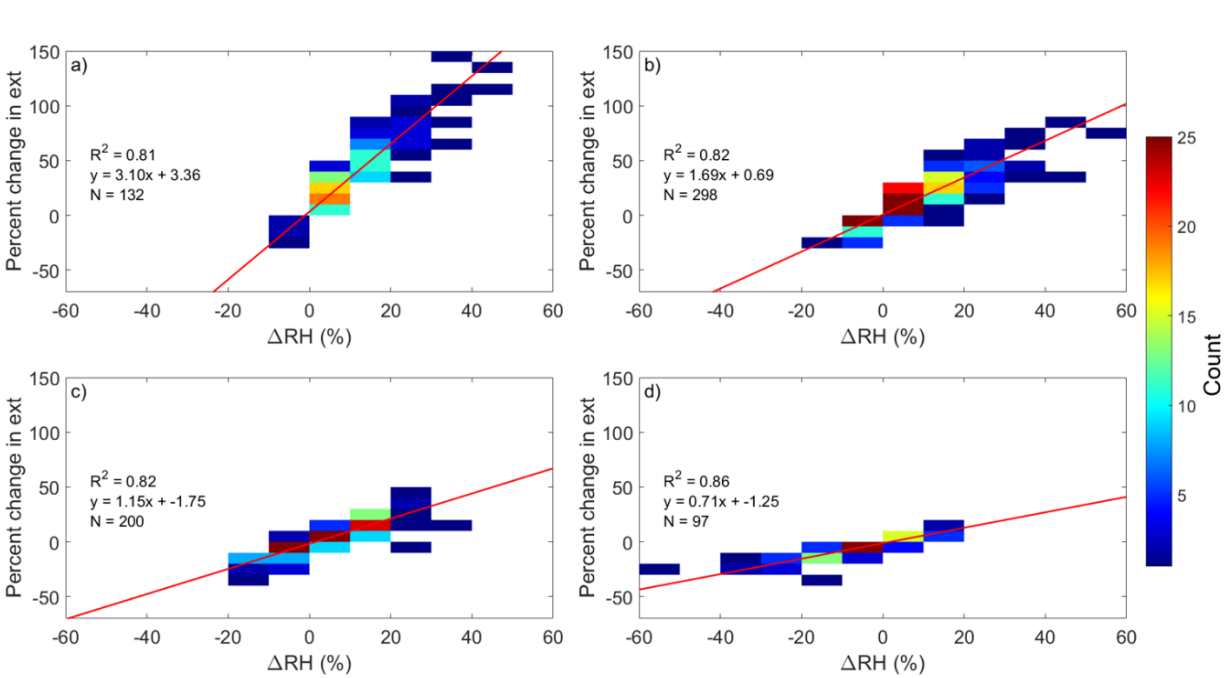

Figure S5. Percent change in the simulated NAAPS-RA 532 nm extinction coefficient versus the difference between dropsonde and NAAPS-RA RH (ΔRH) for each pressure layer when final dropsonde values were (**a**) > 90%, (**b**) between 80 - 90 %, (**c**) between 60 - 80%, and (**d**) < 60 %. Linear fits are indicated with red lines, and the color bar indicates the number of points falling in each bin.

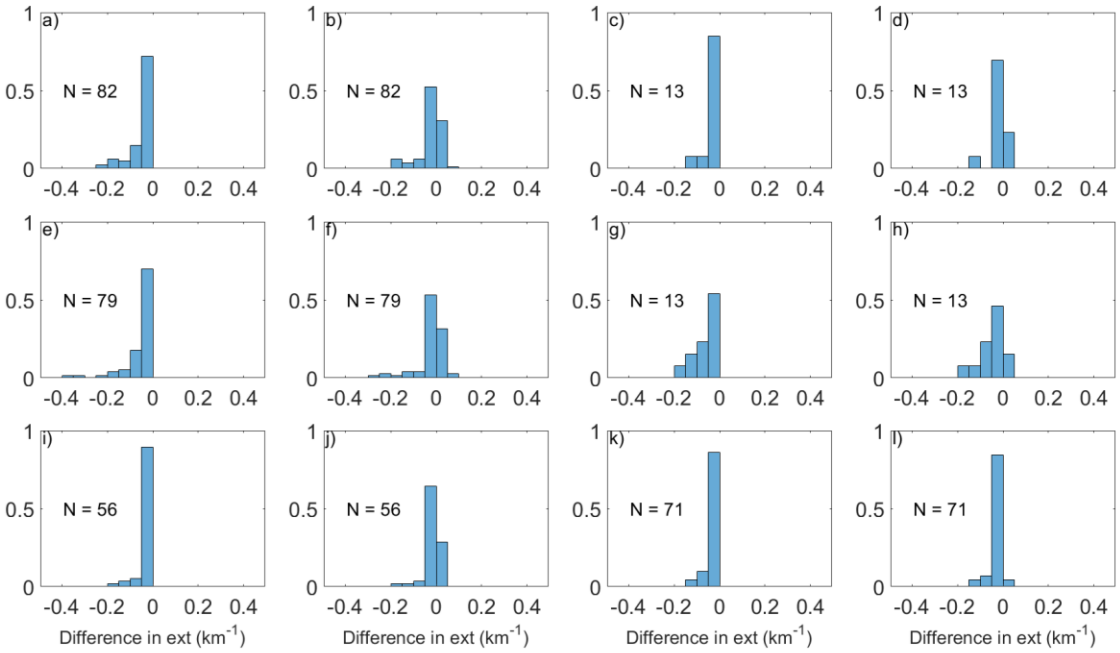

Figure S6. Normalized histograms of differences between simulated (NAAPS-RA) and retrieved (HSRL-2) 532 nm extinction coefficients when NAAPS-RA underestimated both extinction and RH. (**a**,**b**) Differences in extinction when NAAPS-RA simulations were calculated using either (**a**) NAAPS-RA RHs or (**b**) dropsonde RHs for altitudes between 40 – 500 m and when final dropsonde RHs were > 80%. (**c**,**d**) Same as (**a**,**b**, respectively) except when final dropsonde RHs were < 80%. (**e**,**f**) Same as (**a**,**b**, respectively) except for altitudes between 500 – 1500 m. (**g**,**h**) Same as (**e**,**f**, respectively) except when final dropsonde RHs were < 80%. (**i**,**j**) Same as (**a**,**b**, respectively) except for altitudes > 1500 m. (**k**, **l**) Same as (**i**,**j**) except when final dropsonde RHs were < 80%.

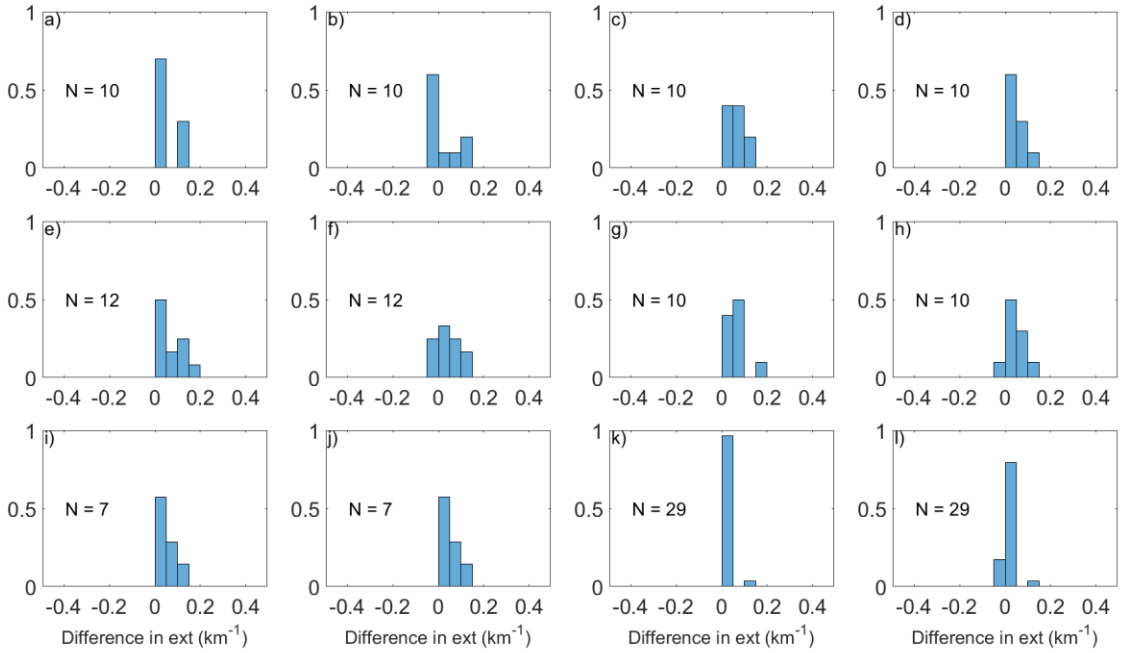

Figure S7. Same as Fig. S6, except when NAAPS-RA overestimated both extinction and RH.

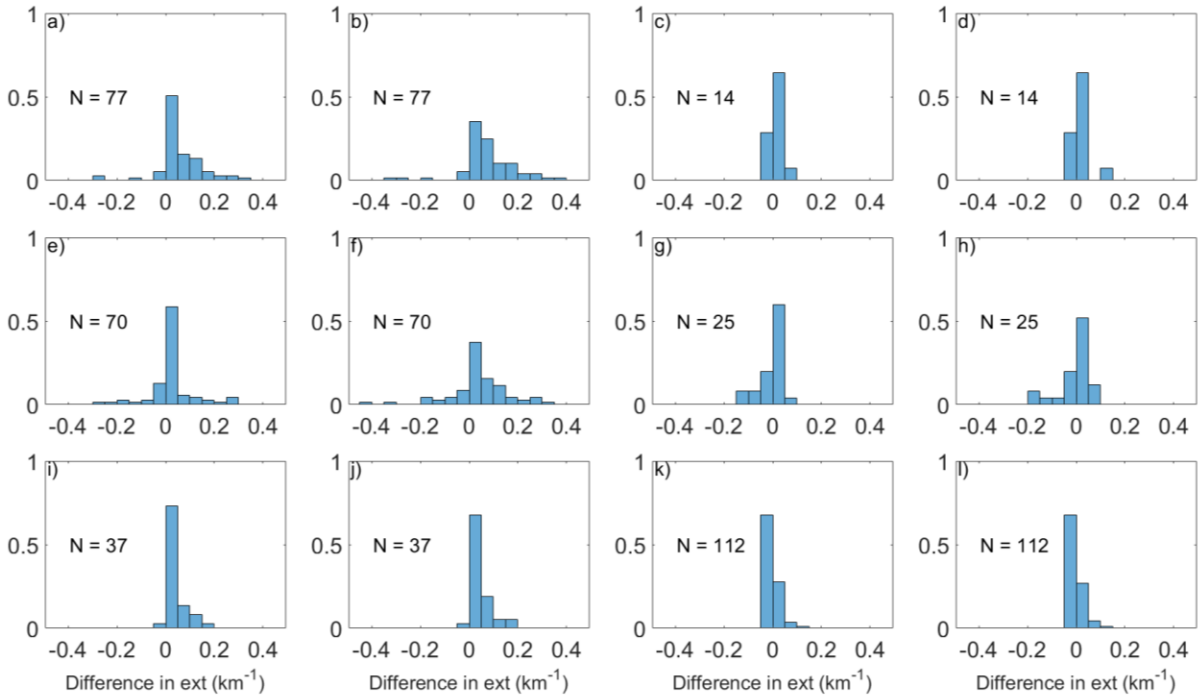

Figure S8. Same as Fig. S6 except when NAAPS-RA either (i) underestimated extinction and overestimated RH or (ii) overestimated extinction and underestimated RH.

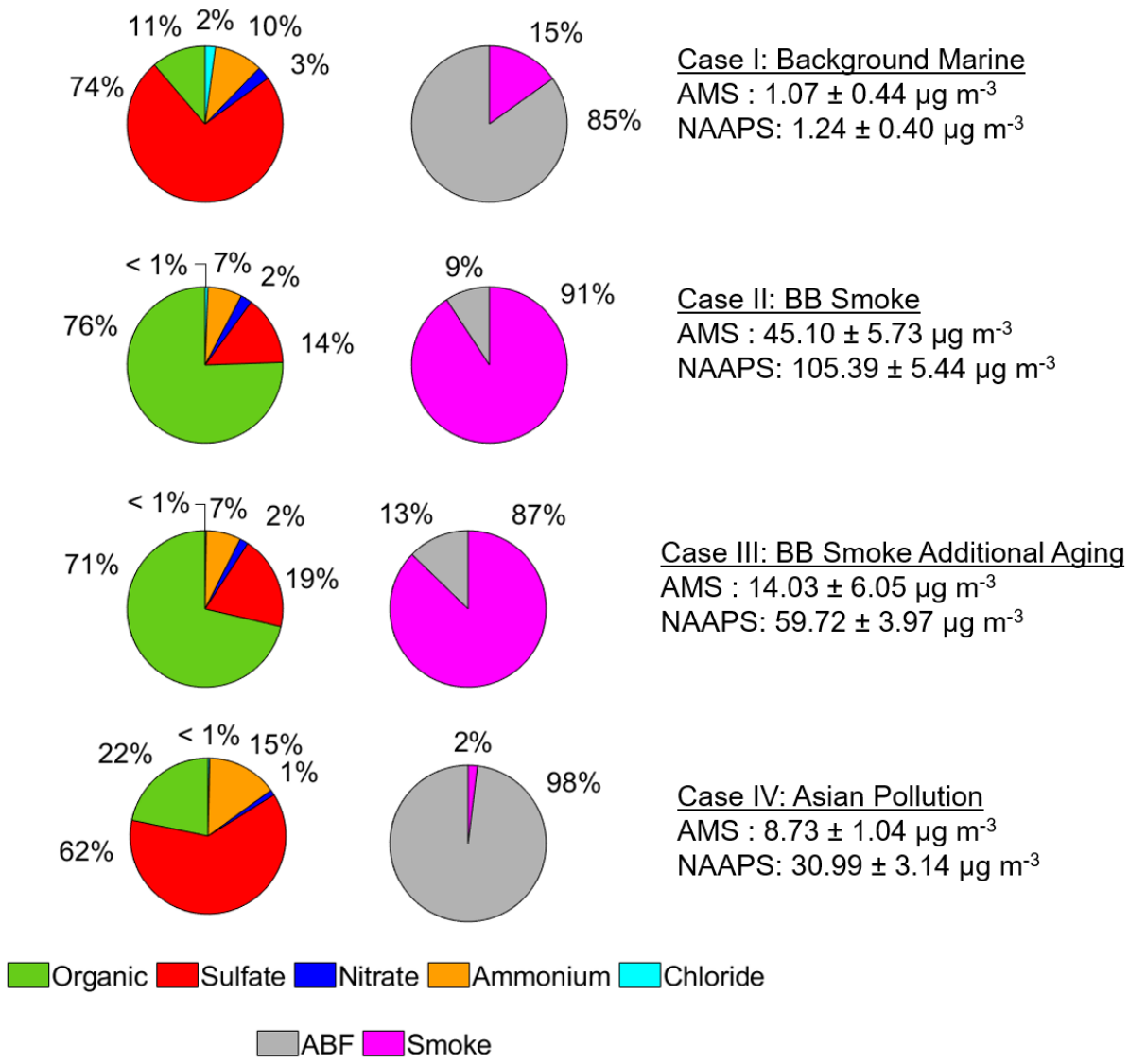

58

59 **Figure S9.** Fine-mode aerosol composition in the ML based on AMS measurements (left) and
60 NAAPS-RA simulations (right) for each case study. Mean total fine mass concentrations are
61 provided to the right of the pie charts. AMS fine mode considers particles 60 – 600 nm, while
62 NAAPS-RA fine mode considers particles < 1000 nm. "BB" stands for biomass burning.

References

Rolph, G., Stein, A., and Stunder, B.: Real-time Environmental Applications and Display sYstem: READY, Environmental Modelling & Software, 95, 210-228, https://doi.org/10.1016/j.envsoft.2017.06.025, 2017.

Stein, A. F., Draxler, R. R., Rolph, G. D., Stunder, B. J. B., Cohen, M. D., and Ngan, F.: NOAA's HYSPLIT Atmospheric Transport and Dispersion Modeling System, Bulletin of the American Meteorological Society, 96, 2059-2077, https://doi.org/10.1175/bams-d-14-00110.1, 2015.